

# Improved scheme for generation of vibrational trio coherent states of a trapped ion

Hyo Seok Yi

Department of Physics, Korea Advanced Institute of Science and Technology,  
373-1 Guseong-dong, Yuseong-gu, Daejeon 305-701, Republic of Korea

Ba An Nguyen\* and Jaewan Kim

School of Computational Sciences, Korea Institute for Advanced Study,  
207-43 Cheongryangni 2-dong, Dongdaemun-gu, Seoul 130-722, Republic of Korea

We improve a previously proposed scheme (Phys. Rev. A 66 (2002) 065401) for generating vibrational trio coherent states of a trapped ion. The improved version is shown to gain a double advantage: (i) it uses only five, instead of eight, lasers and (ii) the generation process can be made remarkably faster.

PACS number: 42.50.Dv

Following the pair coherent state (PCS) [1], which has proved very important in quantum optics [2], atom-field dynamics [3], quantum-mechanics-versus-local-realism test [4], continuous-variable quantum nonlocality [5] and quantum information [6], the so-called trio coherent state (TCS) [7] and their cat-type superpositions [8] have also been introduced recently. This novel family of states has been shown inherently nonclassical exhibiting new types of multimode antibunching, higher-order squeezing and violation of Cauchy-Schwarz inequalities. Although the recognized kinds of nonclassical states have been numerous to date (see, *e.g.* [9]), it is not yet justified that all of them acquire actual applications. It is also not excluded that “really needed” states remain undiscovered or they are among the existing ones with their necessary properties unnoticeable. In that sense, any further detailed study of a known state or introduction of a new state would be perhaps equally welcome. As for the TCS, because of their three-mode nature, they would play a significant role in phenomena in which the PCS could not. For example, with the TCS one might predict that “one-event” continuous-variable local realism violating experiments could be found in a way more or less similar to those devised by Greenberger-Horne-Zeilinger [10] or/and by Hardy [11] for observables with discrete spectra. However, before any expected experiment can be done, a primary question arises: how can one produce the TCS in practice? This question was answered in [7] for electromagnetic fields interacting with an atom when there is strong competition between trio parametric conversion and trio absorption. Here we shall concern with generation of TCS in the center-of-mass motion of a trapped ion. The motivation is that advanced laser-cooling techniques applied to single trapped ions allow to cool them down near their zero-point vibrational energy (see, *e.g.*, Ref. [12]). In that quantized regime, the ion vibrational modes can be looked upon as ideal bosons which are almost uninfluenced by the environment resulting in negligible decoherences. This fact greatly favors potential implementations such as designing quantum logic gates in a quantum computer [13] (in particular, the controlled-NOT gate has been realized in two  $^{40}\text{Ca}^+$  ions in a Paul trap individually radiated by focused lasers [14]). Laser-driven trapped ions placed inside optical cavities can also entangle the cavity mode simultaneously with the internal and external degrees of freedom of the ion [15]. Previously, the vibrational TCS in a 3D trap was shown to be generated by a scheme using eight lasers [16] (compare with schemes for the vibrational PCS in a 2D trap [17]). In this Letter we shall improve the scheme proposed in [16] by reducing the number of used lasers from eight to five. Moreover, we shall carry out detailed simulation to reveal that the time needed to generate the vibrational TCS can be made shorter in the improved version than in the original one [16].

The vibrational TCS, denoted by  $|\xi, p, q\rangle$  with  $\xi = r \exp(i\varphi)$  and  $p, q$  integers, is a three-mode entangled continuous superposition of coherent states of the form

$$|\xi, p, q\rangle = \frac{N(p, q, r) \exp(3r^{2/3}/2)}{\xi^{(p+q)/3}} \times \int_0^{2\pi} \frac{d\theta}{2\pi} \int_0^{2\pi} \frac{d\theta'}{2\pi} \exp[-i(q\theta + p\theta')] \times \left| \xi^{1/3} \exp(i\theta) \right)_x \left| \xi^{1/3} \exp(i\theta') \right)_y \left| \xi^{1/3} \exp[-i(\theta + \theta')] \right)_z \quad (1)$$

---

\*Corresponding author. Email: nbaan@kias.re.kr

where  $N(p, q, r)$  defined by

$$N(p, q, r)^{-2} = \sum_{n=0}^{\infty} \frac{r^{2n}}{(n+q)!(n+p)!n!} \quad (2)$$

is the normalization coefficient and  $|... \rangle_{x(y,z)}$  stand for coherent states in the vibrational mode along the  $x$  ( $y, z$ ) axis with the annihilation boson operators  $\hat{a}_{x(y,z)}$ . Equivalently, the state  $|\xi, p, q\rangle$  can also be represented in terms of correlated boson number trios as

$$|\xi, p, q\rangle = \sum_{n=0}^{\infty} C_n(\xi, p, q) |n+q\rangle_x |n+p\rangle_y |n\rangle_z \quad (3)$$

where

$$C_n(\xi, p, q) = \frac{N(p, q, r)\xi^n}{\sqrt{(n+q)!(n+p)!n!}} \quad (4)$$

and  $|... \rangle_{x(y,z)}$  stand for Fock states in the  $x$  ( $y, z$ ) axis mode. Both the representations (1) and (3) come from the fact that the vibrational TCS is defined as the joint eigenstate of the operators  $\hat{a}_x \hat{a}_y \hat{a}_z$ ,  $\hat{P} = \hat{a}_y^+ \hat{a}_y - \hat{a}_z^+ \hat{a}_z$  and  $\hat{Q} = \hat{a}_x^+ \hat{a}_x - \hat{a}_z^+ \hat{a}_z$ , *i.e.*

$$\hat{a}_x \hat{a}_y \hat{a}_z |\xi, p, q\rangle = \xi |\xi, p, q\rangle, \quad (5)$$

$$\hat{P} |\xi, p, q\rangle = p |\xi, p, q\rangle, \quad (6)$$

$$\hat{Q} |\xi, p, q\rangle = q |\xi, p, q\rangle. \quad (7)$$

Generally, the system of a two-level ( $|g\rangle$  and  $|e\rangle$  : ground and excited state) ion localized in a small region by a 3D isotropic harmonic potential and radiated by  $L$  external lasers is described by the Hamiltonian ( $\hbar = 1$ )

$$H = H_0 + H_{int}, \quad (8)$$

$$H_0 = \frac{1}{2} \Delta \sigma_z + \sum_{j=x,y,z} \nu \left( \hat{a}_j^+ \hat{a}_j + \frac{1}{2} \right), \quad (9)$$

$$H_{int} = \sum_{l=1}^L [\Omega_l \exp[i(\omega_l t + \phi_l)] g_l \sigma_- + \text{H.c.}] \quad (10)$$

with  $\Delta$  the energy gap between the ion's two levels,  $\sigma_- = |g\rangle \langle e| = \sigma_+^+$ ,  $\sigma_z = |e\rangle \langle e| - |g\rangle \langle g|$ ,  $\nu$  the energy of a quantum of the vibrational motion,  $\Omega_l$  the Rabi frequencies,  $\omega_l$  ( $\phi_l$ ) the laser frequencies (phases) and  $g_l$  the laser spatial profile. For travelling waves  $g_l = \exp[-i\mathbf{k}_l \mathbf{R}_l]$  with  $\mathbf{R}_l$  the position operators along the laser propagation directions determined by the wave vectors  $\mathbf{k}_l$ . Instead of 8 lasers as proposed in [16], here we use only 5 lasers. The first four lasers are directed as sketched in Fig. 1, each of which is detuned to the third lower sideband of the ion vibrational motion, *i.e.*  $\omega_{l=1,2,3,4} = \Delta - 3\nu$ . As for the fifth laser, its direction is unimportant but its frequency must be in resonant with the ion transition, *i.e.*  $\omega_{l=5} = \Delta$ . Assuming an equal wave number for all the lasers we are left with a unique Lamb-Dicke parameter  $\eta$  which is a measure of the ion's localization region compared with the laser wavelength. If  $\nu$  is much larger than any other characteristic frequencies (resolved sideband limit) and  $\eta \ll 1$  (Lamb-Dicke limit), we have, in the interaction picture and in leading order in  $\eta$ , the interaction Hamiltonian of the form [16]

$$\mathcal{H}_{int} = \left[ -\frac{i\eta^3}{6} \sum_{l=1}^4 \Omega_l e^{-i\phi_l} \hat{A}_l^3 + \Omega_5 e^{-i\phi_5} \right] \sigma_+ + \text{H.c.} \quad (11)$$

where the annihilation operators of the vibration quanta in the direction  $\mathbf{R}_l$  are denoted by  $\hat{A}_l$  which are related to  $\hat{a}_{x(y,z)}$  as

$$\hat{A}_1 = \hat{a}_x + \hat{a}_y + \hat{a}_z, \quad \hat{A}_2 = \hat{a}_x - \hat{a}_y + \hat{a}_z, \quad (12)$$

$$\hat{A}_3 = \hat{a}_x + \hat{a}_y - \hat{a}_z, \quad \hat{A}_4 = \hat{a}_x - \hat{a}_y - \hat{a}_z. \quad (13)$$

If we now adjust the laser intensity and phase to meet the conditions  $\Omega_{l=1,2,3,4} = \Omega$  and  $\phi_{l=1,3} = \phi_{l=2,4} + \pi = \phi$ , then the Hamiltonian (11) simplifies to

$$\mathcal{H}_{int} = \zeta (\hat{a}_x \hat{a}_y \hat{a}_z - \xi) \sigma_+ + \text{H.c.}$$

with  $\zeta$  and  $\xi$  determined by the system parameters in a controllable manner as

$$\zeta = -6i\eta^3\Omega \exp[-(i\phi + \eta^2/2)], \quad (14)$$

$$\xi = -\frac{i\Omega_5}{6\Omega\eta^3} \exp[i(\phi - \phi_5)]. \quad (15)$$

Because the damping of vibrational quanta is negligible, the main decay process occurs via ionic spontaneous emission with rate  $\gamma$ . Thus, in the Lamb-Dicke limit, the system density operator  $\rho$  obeys the master equation [16]

$$\frac{d\rho}{dt} = -i[\mathcal{H}_{int}, \rho] - \frac{\gamma}{2} (\sigma_+ \sigma_- \rho + \rho \sigma_+ \sigma_- - 2\sigma_- \rho \sigma_+). \quad (16)$$

In the long-time limit, Eq. (16) has a “dark” steady solution  $\rho_s = |g\rangle |\Psi\rangle \langle \Psi| \langle g|$  with  $|\Psi\rangle$  responsible for the steady state of the ion vibration. It is easy to verify that  $|\Psi\rangle$  obeys the equation

$$\hat{a}_x \hat{a}_y \hat{a}_z |\Psi\rangle = \xi |\Psi\rangle. \quad (17)$$

Further, if the ion is initially prepared in a Fock state  $|\Psi_0\rangle = |q+k\rangle_x |p+k\rangle_y |k\rangle_z$  with  $k$  a non-negative integer, then, because  $p$  and  $q$  are conserved in the problem under treatment, the state  $|\Psi\rangle$  satisfies also the two equations

$$\hat{P} |\Psi\rangle = p |\Psi\rangle, \quad (18)$$

$$\hat{Q} |\Psi\rangle = q |\Psi\rangle. \quad (19)$$

Comparing (17) - (19) with (5) - (7) yields  $|\Psi\rangle \equiv |\xi, p, q\rangle$  which is the vibrational TCS we want to generate.

To follow the transient process and to assess generation time (*i.e.* the time needed for the system to reach the steady regime) we simulate Eq. (16) by the Monte Carlo Wave-Function approach [18]. The system wave function at time  $t$  is looked for in the form

$$\Phi(t) = \sum_{l,m,n} [G_{lmn}(t) |g\rangle + E_{lmn}(t) |e\rangle] |l\rangle_x |m\rangle_y |n\rangle_z. \quad (20)$$

For the purpose of numerical calculation, the Fock-state basis should be confined to  $l, m, n \leq N_{\max}$  with  $N_{\max}$  a cutoff to be chosen such that its increasing does not change the result within a pre-set high enough accuracy. In our simulations we have found  $N_{\max} = 10$  sufficient for most of the numerical calculation: just an error of less than  $10^{-6}$  arises by increasing the cutoff by one. For convenience, we use the dimensionless time  $\tau$  determined by  $\tau = \gamma t$ . For the initial condition  $\Phi(0) = |e\rangle |q+k\rangle_x |p+k\rangle_y |k\rangle_z$  with  $k = 4$ , the time evolution of the probability  $P(l, m, n) = |G_{lmn}|^2 + |E_{lmn}|^2$  of finding the ion in a Fock state  $|l\rangle_x |m\rangle_y |n\rangle_z$  is plotted in Fig. 2a. As is visual from that figure, at the beginning  $P(l, m, n)$  oscillate but at large  $\tau$  they approach  $|C_n(\xi, p, q)|^2$  (see Eq. (4)) precisely, implying generation of the vibrational TCS. The initial variation of  $P(l, m, n)$  depends on the value of  $k$  but their long-time behavior is  $k$ -independent. This means that the TCS is eventually generated independently of the choice of  $k$  which is best taken as  $k = 0$  because the state  $|e\rangle |q\rangle_x |p\rangle_y |0\rangle_z$  is easiest to prepare practically. The transition towards the steady regime can be watched as well in Fig. 2b showing how the inversion  $\langle \sigma_z \rangle = \sum_{l,m,n} (|E_{lmn}|^2 - |G_{lmn}|^2)$  evolves from 1 to -1. The purity of the generated state is examined by the fidelity  $F(\tau) = |\langle \Phi(\tau) | \xi, p, q \rangle|^2$  whose

change in time is depicted in Fig. 3. Because of the truncation in the Fock basis we determine the vibrational TCS generation time  $\tau_s$  by the constraint  $1 - F(\tau_s) = 10^{-5}$  and display the  $\tau_s$  as a function of  $\alpha = \zeta/\gamma$  in Fig. 4a. The decreasing of  $\tau_s$  with increasing  $\alpha$  plays a role as will be seen.

Finally, we discuss a possibility to make the generation time in the present improved scheme ( $L = 5$  scheme) shorter than that in the previous scheme ( $L = 8$  scheme) [16]. Suppose we wish to produce a state  $|\xi, p, q\rangle$  with fixed  $\xi$ ,  $p$  and  $q$ . The desired values of  $p$  and  $q$  are easily to manage by preparing an initial state in the form  $|e\rangle|q+n\rangle_x|p+n\rangle_y|n\rangle_z$  with  $n$  a non-negative integer. To tailor  $\xi$  we use Eq. (10) of Ref. [16] and Eq. (15) of this work. The same value of  $\xi$  in the  $L = 8$  scheme can be obtained in the  $L = 5$  scheme in either of the two following ways: (i) keeping the frequency of the 5th laser in the  $L = 5$  scheme equal to that of the 8th laser in the  $L = 8$  scheme, but decreasing the frequencies of the 1st to 4th laser in the  $L = 5$  scheme 6 times smaller than those of the 1st to 7th laser in the  $L = 8$  scheme or (ii) increasing the frequency of the 5th laser in the  $L = 5$  scheme 6 times larger than that of the 8th laser in the  $L = 8$  scheme, but keeping the frequencies of the 1st to 4th laser in the  $L = 5$  scheme equal to those of the 1st to 7th laser in the  $L = 8$  scheme. In case (i) the value of  $\zeta$  in the  $L = 5$  scheme (see Eq. (14) of this work) remains unchanged in comparison with that in the  $L = 8$  scheme (see the equation before Eq. (10) in Ref. [16]) and, hence, both schemes undergo the same dynamics. Nevertheless, if case (ii) is chosen, the value of  $\zeta$  in the  $L = 5$  scheme becomes 6 time larger than that in the  $L = 8$  scheme. Since  $\tau_s$ , for the same value of  $\gamma$ , decreases with increasing  $\zeta$  (see Fig. 4a), a net advantage in the generation time appears in the improved scheme. Figure 4b shows that advantage from an angle of the  $\xi$ -dependence, for more clarity. A noteworthy merit of the  $L = 5$  scheme is that, for the whole range of  $\xi$ , the desired TCS is generated in a remarkably shorter time compared with the  $L = 8$  scheme.

In summary, we have improved a recently proposed scheme for generating trio coherent states in the vibrational motion of an ion trapped in three dimensions. The trio coherent state generated by this scheme is stable because it appears in a steady regime in which the ion has fully relaxed to its ground “dark” state (Fig. 2b) which is identified by the quenched fluorescence from the ion. Besides reduction in the number of driving lasers to be used, the improved version can also provide a much shorter generation time. The possibility to shorten the generation time  $\tau_s$  relies upon its decrease with increasing  $\alpha$ . In general, such a decreasing behavior does not exist for the whole range of  $\alpha$ . In fact,  $\tau_s$  would turn out to increase with  $\alpha$ , say, when  $\alpha$  is very large. For instance, in the extreme limit of  $\alpha \rightarrow \infty$  (corresponding to negligible spontaneous emission,  $\gamma \rightarrow 0$ ), periodic oscillations or phenomena like collapses and revivals, undamped self-pulsing or even chaos would occur. However, in problems like the one under consideration, where relaxation to a steady state within a finite time is important,  $\gamma$  is essential and cannot be treated as arbitrarily small and, thus, arbitrarily large values of  $\alpha$  are irrelevant. To specify the range of  $\alpha$  for which our simulations have been carried out, we use  $\eta$  as a measure of smallness since  $\eta \ll 1$  in the Lamb-Dicke limit we are working in. As explained, because the ionic decay cannot be neglected, let us be interested in situations such that  $\gamma$  satisfies the condition  $\gamma/(6\Omega) \gg \mathcal{O}(\eta^3)$ . Then, from Eq. (14), we get  $\alpha = \zeta/\gamma \simeq \mathcal{O}(6\Omega\eta^3/\gamma)$  which is much less than unity. For smaller values of  $\gamma$  (*i.e.* larger  $\alpha$ ), as mentioned above, abundant dynamics associated with other different timescales will take place which should be dealt with separately (*e.g.*, by means of multiple-timescale analyses).

### Acknowledgments

The authors thank the KIAS Quantum Information Group for useful discussions. H.S.Y. is supported by a KAIST Grant for Basic Science, B.A.N. by a KIAS Research Fund (No. 02-0149-001) and J.K. by a Korea Research Foundation Grant (KRF-2002-070-C00029).

---

- [1] G. S. Agarwal, Phys. Rev. Lett. 57 (1986) 827;  
G. S. Agarwal, J. Opt. Soc. Am. B 5 (1988) 1940.
- [2] Ts. Gantsog and R. Tanas, Opt. Commun. 82 (1991) 145;  
B. A. Bambah and G. S. Agarwal, Phys. Rev. A 51 (1995) 1698;  
A. Gilchrist and W. J. Munro, J. Opt. B: Quantum Semiclass. Opt. 2 (2000) 47;  
Arvind, Phys. Lett. A 299 (2002) 461.
- [3] A. Joshi and R. R. Puri, Phys. Rev. A 42 (1990) 4336;  
S. C. Gou, Phys. Rev. A 48 (1993) 3233.
- [4] K. Tara and G. S. Agarwal, Phys. Rev. A 50 (1994) 2870;  
A. Gilchrist, P. Deuar and M. D. Reid, Phys. Rev. Lett. 80 (1998) 3169;  
W. J. Munro, Phys. Rev. A 59 (1999) 4197;  
A. Gilchrist, P. Deuar and M. D. Reid, Phys. Rev. A 60 (1999) 4259.

- [5] S. Mancini, V. I. Manko, E. V. Shchukin and P. Tombesi, e-print quant-ph/0302089.
- [6] S. Mancini and P. Tombesi, Quant. Inf. and Comp. 3 (2003) 106.
- [7] B. A. Nguyen and M. D. Truong, J. Opt. B: Quantum Semiclass. Opt. 4 (2002) 80;  
B. A. Nguyen, J. Opt. B: Quantum Semiclass. Opt. 4 (2002) 222.
- [8] B. A. Nguyen and M. D. Truong, J. Opt. B: Quantum Semiclass. Opt. 4 (2002) 289;  
B. A. Nguyen, Phys. Lett. A 311 (2003) in press.
- [9] V. V. Dodonov, J. Opt. B: Quantum Semiclass. Opt. 4 (2002) R1.
- [10] D. M. Greenberger, M. A. Horne and A. Zeilinger, in *Bell's Theorem, Quantum Theory and Conceptions of the Universe*, ed. M. Kafatos (Kluwer Academic, Dordrecht, 1989);  
N. D. Mermin, Am. J. Phys. 58 (1990) 731;  
B. Yurke and D. Stoler, Phys. Rev. Lett. 68 (1992) 1251.
- [11] L. Hardy, Phys. Rev. Lett. 68 (1992) 2981;  
L. Hardy, Phys. Lett. A 167 (1992) 17.
- [12] C. Monroe *et al.*, Phys. Rev. Lett. 75 (1995) 4011.
- [13] J. I. Cirac and P. Zoller, Phys. Rev. Lett. 74 (1995) 4091;  
C. Monroe *et al.*, Phys. Rev. A 55 (1997) R2489;  
F. Poyatos, J. I. Cirac and P. Zoller, Phys. Rev. Lett. 81 (1998) 1322;  
J. A. Sorensen and K. Molmer, Phys. Rev. A 62 (2000) 022311;  
A. M. Chids and I. L. Chuang, Phys. Rev. A 63 (2000) 012306.
- [14] F. Schmidt-Kaler *et al.*, Nature 422 (2003) 408.
- [15] A. B. Mundt *et al.*, Appl. Phys. B 76 (2003) 117;  
S. S. Sharma, Phys. Lett. A 311 (2003) 111.
- [16] B. A. Nguyen and M. D. Truong, Phys. Rev. A 66 (2002) 065401.
- [17] S. C. Gou, J. Steinbach and P. L. Knight, Phys. Rev. A 54 (1996) R1014;  
W. Kaige *et al.*, Phys. Rev. A 63 (2001) 043419.
- [18] J. Dalibard, Y. Castin and K. Molmer, Phys. Rev. Lett. 68 (1992) 580.

### Figure captions

Fig. 1: The configuration of used lasers : the 1st (2nd, 3rd and 4th) laser propagates along the direction connecting the coordinate origin “o” with the point with  $\{x, y, z\} = \{1, 1, 1\}$  ( $\{1, -1, 1\}$ ,  $\{1, 1, -1\}$  and  $\{1, -1, -1\}$ ), while the 5th laser can be oriented arbitrarily (not shown).

Fig. 2: a) Left: The probability  $P(l, m, n)$  *versus* scaled time  $\tau = \gamma t$  for the initial condition  $\Phi(0) = |e\rangle |q+4\rangle_x |p+4\rangle_y |4\rangle_z$ . The parameters used are  $\alpha = 0.02$ ,  $\xi = 2.0$ ,  $p = 3$  and  $q = 2$ . The values of  $l, m, n$  are indicated by  $(l, m, n)$ . All the  $P(l, m, n)$  with  $m \neq n + p$  and  $l \neq n + q$  are identically zeros, whereas all the  $P(q + n, p + n, n)$  with  $n \geq 3$  are negligible in the long-time limit. Right: Distribution of  $|C_n(\xi, p, q)|^2$  (see Eqs. (3) and (4)) for the same values of  $\xi$ ,  $p$  and  $q$  as above. The values of  $n$  are indicated by  $(n)$ . All the  $|C_n(\xi, p, q)|^2$  with  $n \geq 3$  are negligibly small. b) Time evolution of the ionic inversion  $\langle \sigma_z \rangle$  for the same initial condition and parameters as in a). The inset enlarges the variation for the interval  $\tau \in [0, 20]$ .

Fig. 3: Fidelity  $F$  as a function of  $\tau$  for  $\xi = 2.0$ ,  $p = 3$ ,  $q = 2$  and  $\alpha = 0.01, 0.02, 0.03$  (curves indicated by “a”, “b”, “c”, respectively).

Fig. 4: a) The generation time  $\tau_s$  as a function of  $\alpha$  for  $\xi = 2.0$ ,  $p = 3$  and  $q = 2$ . b) As in a) but in logarithmic scale and as a function of  $\xi$  in the  $L = 8$  and  $L = 5$  schemes. Here we use  $\alpha = 0.02$  in the  $L = 8$  scheme which corresponds to  $\alpha = 0.12$  in the  $L = 5$  scheme.

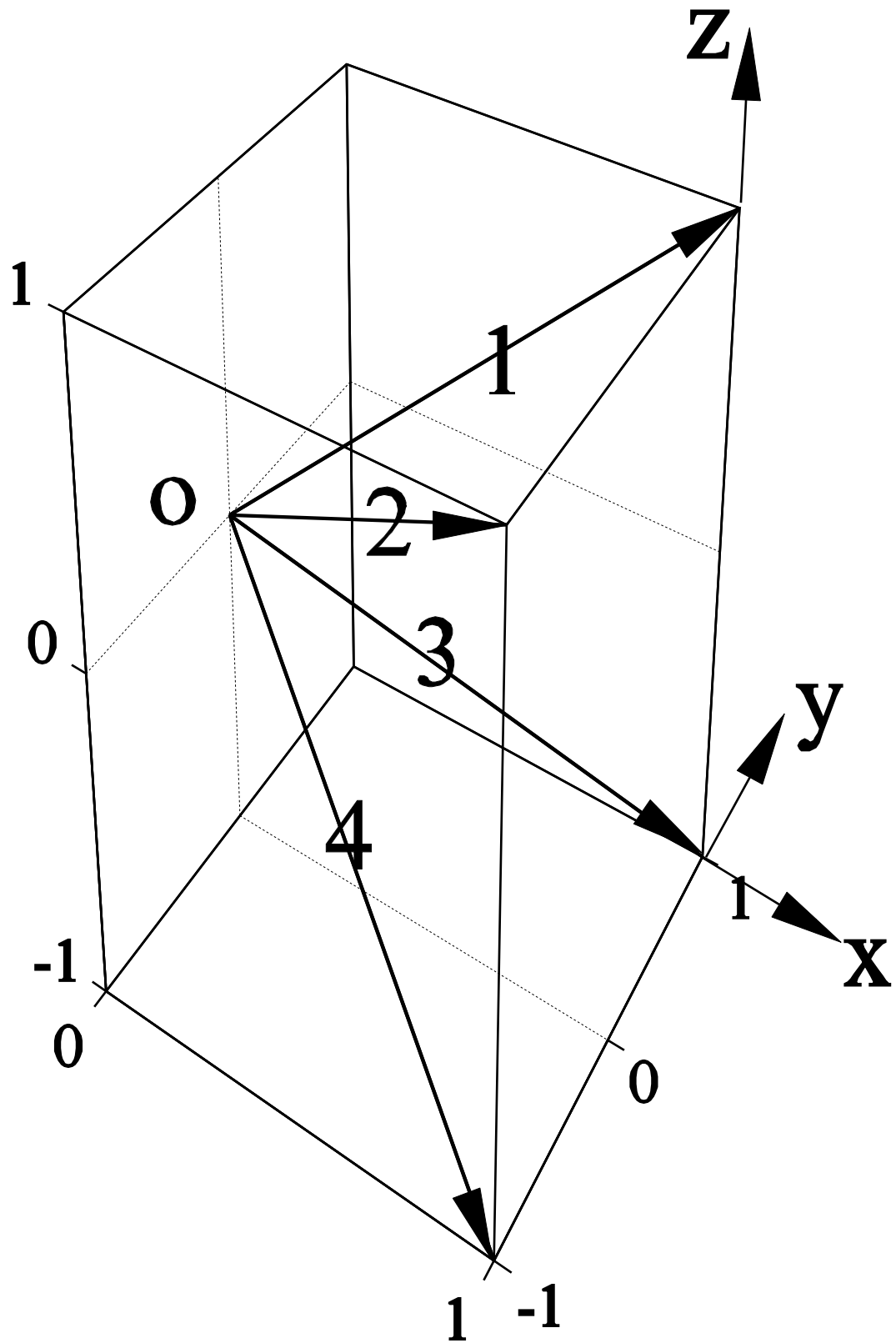


Fig. 1, Yi et al.

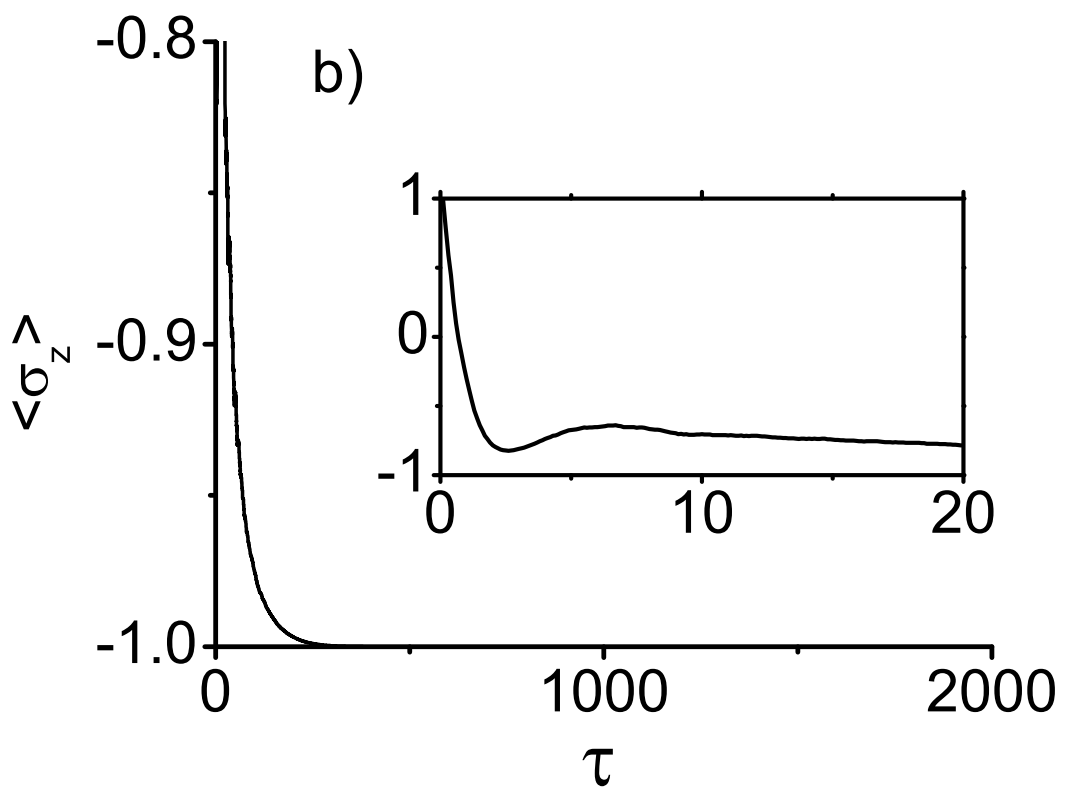
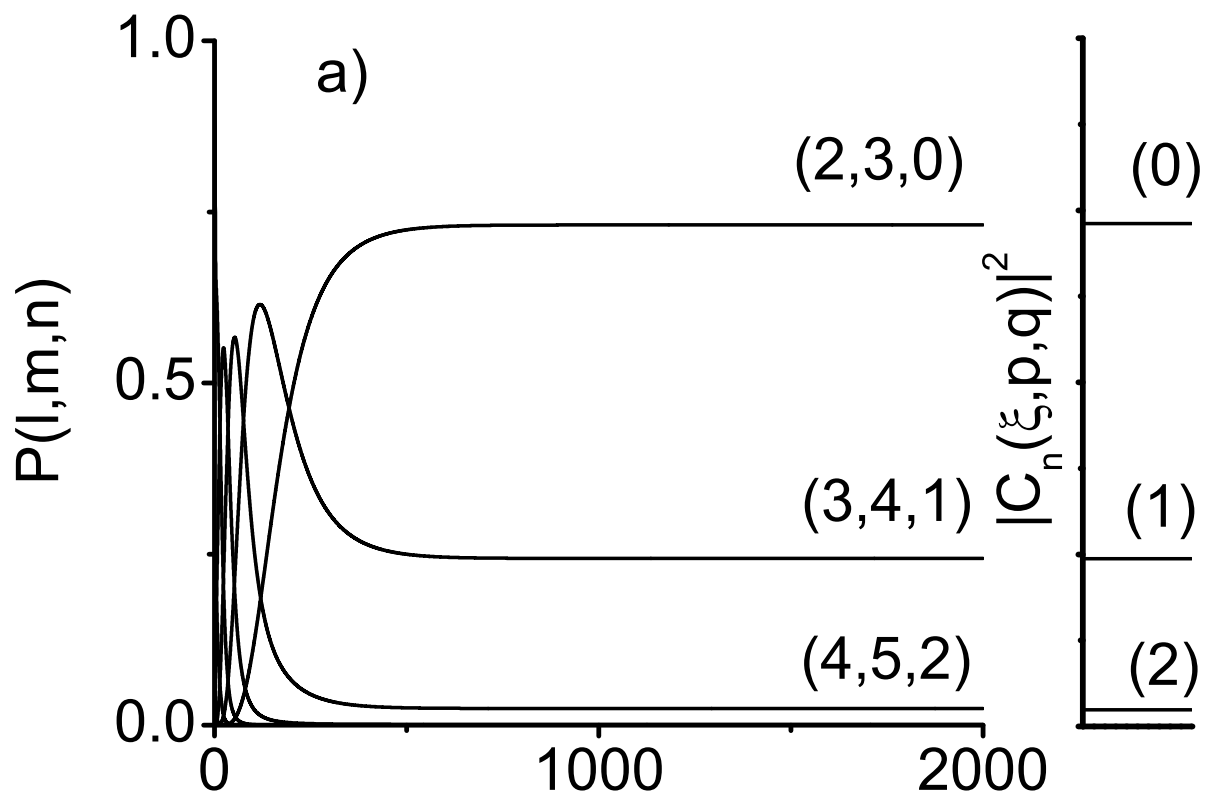


Fig. 2, Yi et al.

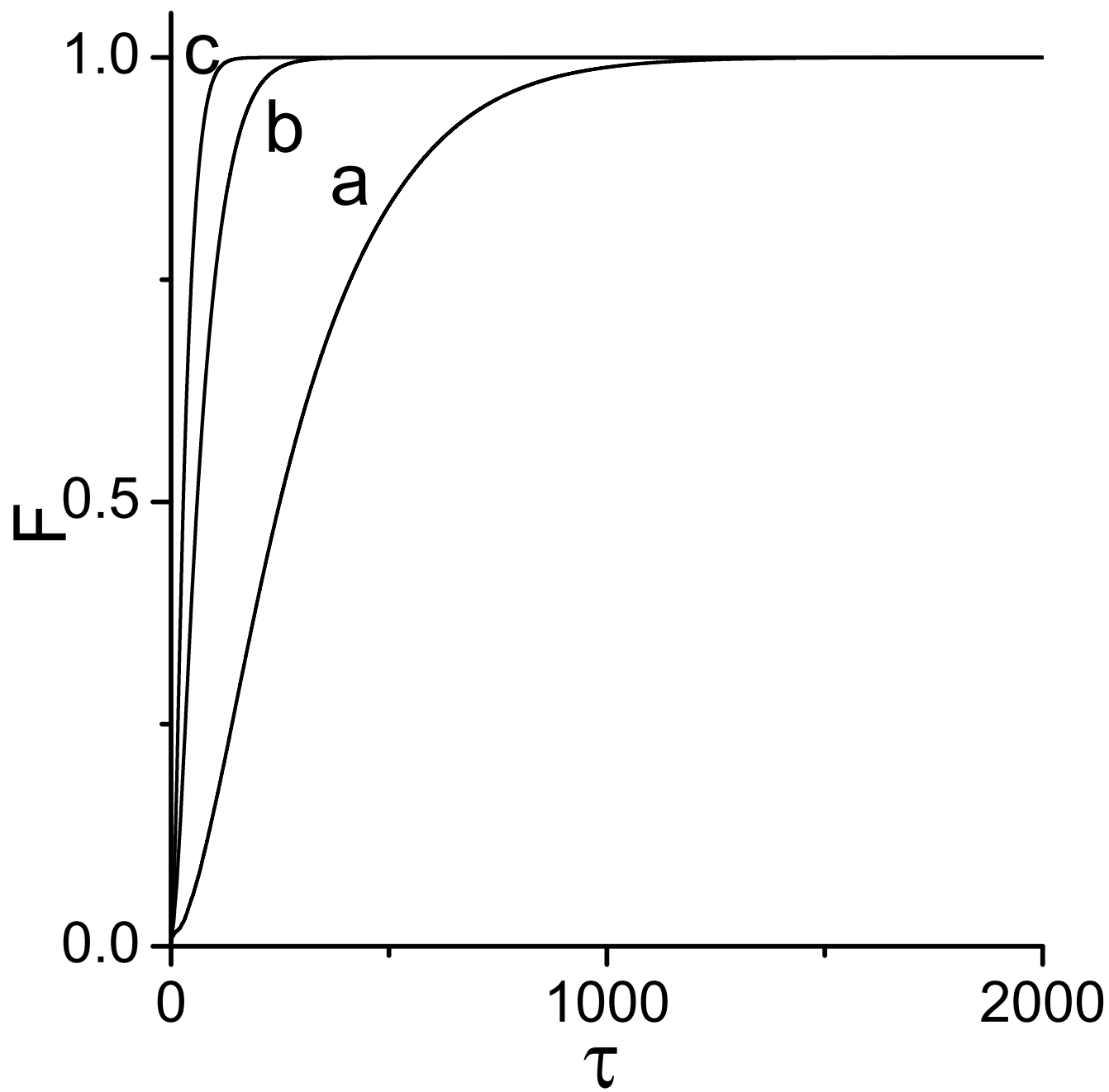


Fig. 3, Yi et al.

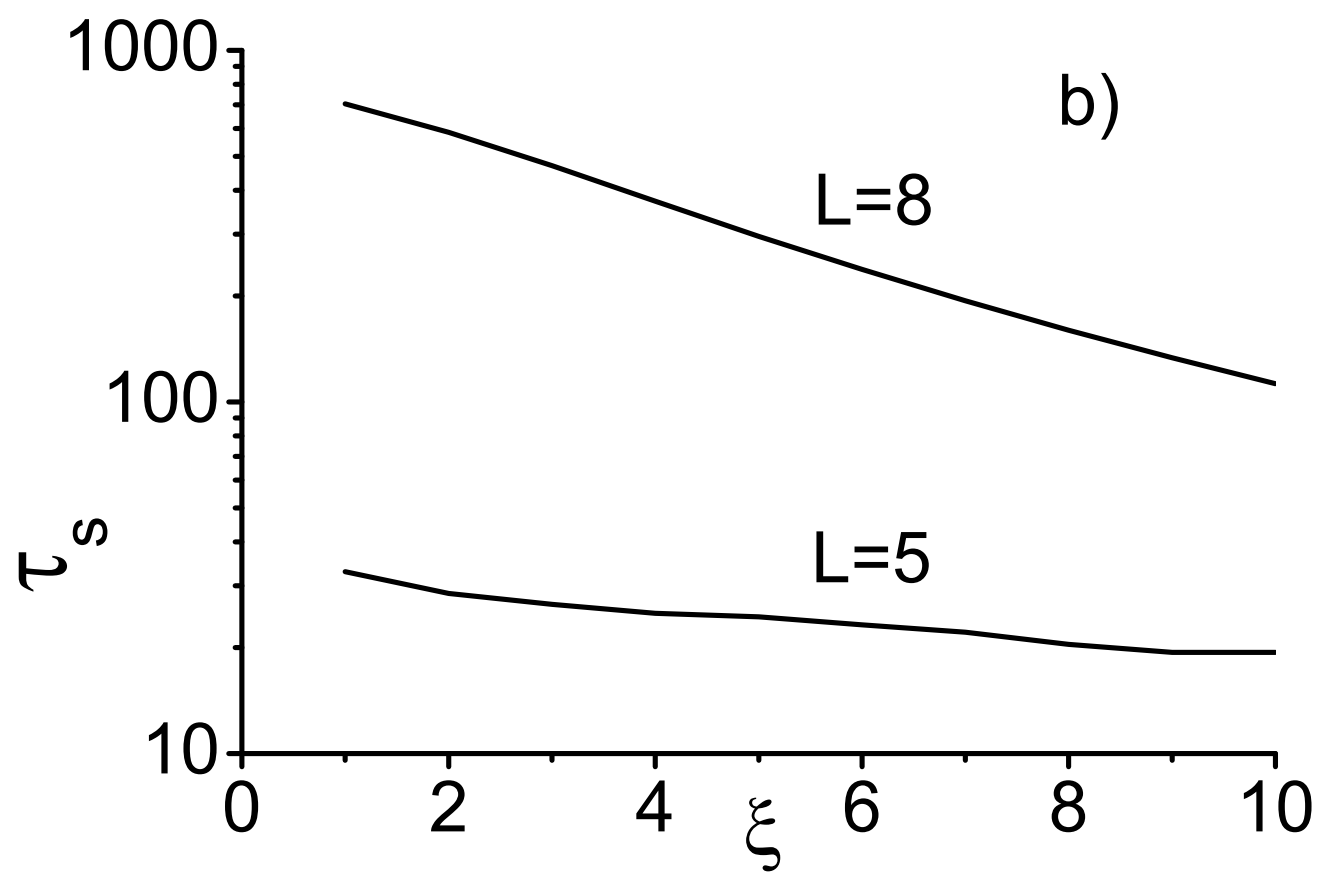
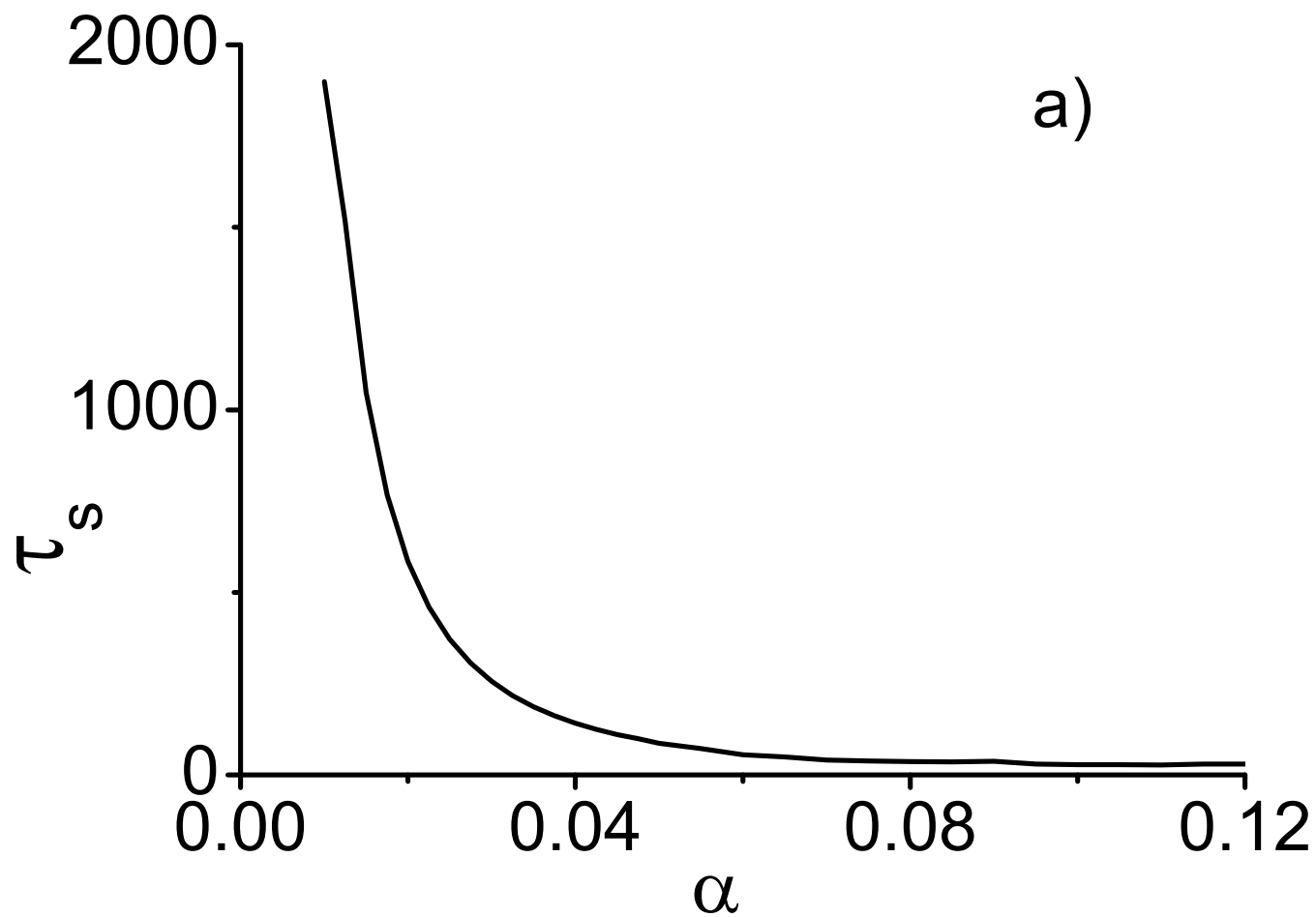


Fig. 4, Yi et al.